Agriculture, Ecosystems and Environment 266 (2018) 68–75

Contents lists available at ScienceDirect

Agriculture, Ecosystems and Environment

journal homepage: www.elsevier.com/locate/agee

Response of soil detachment capacity to plant root and soil properties in typical grasslands on the Loess Plateau

Bing Wang[a,c,*], Guang-Hui Zhang[b], Yan-Fen Yang[a], Pan-Pan Li[a], Jia-Xin Liu[a]

[a] State Key Laboratory of Soil Erosion and Dryland Farming on the Loess Plateau, Institute of Soil and Water Conservation, Northwest A&F University, Yangling, Shaanxi, 712100, PR China
[b] Faculty of Geographical Science, Beijing Normal University, Beijing, 100875, PR China
[c] University of Chinese Academy of Sciences, Beijing, 100049, China

ARTICLE INFO

Keywords:
Soil detachment capacity
Root mass density
Grassland
Overland flow
The Loess Plateau

ABSTRACT

It is likely that grassland has a significant effect on the process of soil detachment by overland flow. This study tests how soil detachment capacity responds to variation in plant root and soil properties between ten typical grasslands found on the Loess Plateau. 300 soil samples were collected from five grasslands with tap root system and five grasslands with fibrous root systems representing the typical community compositions of different succession stages, then subjected to flow scouring in a hydraulic flume under six shear stresses (ranged from 4.98 to 16.37 Pa). The results showed that the mean soil detachment capacity of each grassland fell between 0.030 kg $m^{-2} s^{-1}$ (*Poa sphondylodes* Trin.) and 3.297 kg $m^{-2} s^{-1}$ (*Astragalus melilotoides* Pall.). The mean soil detachment capacity across all grasslands with tap root systems was 14.7 times greater than that of grasslands with fibrous root systems, indicating that fibrous root systems are significantly more effective at reducing soil erosion. Soil detachment capacity was effectively simulated by power functions of flow velocity, shear stress, or stream power (with mean R^2 values ranging from 0.87 to 0.90) and less effectively simulated by a power function of unit stream power (mean $R^2 = 0.74$). Soil detachment capacity decreased exponentially with soil bulk density, aggregate, and cohesion (with R^2 values ranging from 0.87 to 0.99) as well as with root mass density ($R^2 = 0.31$, $n = 150$ for tap root systems and $R^2 = 0.17$, $n = 150$ for fibrous root systems). Soil detachment was significantly worse in grasslands with tap root systems where the root mass density was less than 4 kg m^{-3}. A model was developed to estimate soil detachment capacity based on hydraulic parameters, plant root, and soil properties on the Loess Plateau, and its performance was satisfactory ($R^2 = 0.86$; $NSE = 0.73$). Root mass density, soil aggregate, and soil cohesion were indicated as the primary features of grasslands which influencing the process of soil detachment.

1. Introduction

Vegetation generally has a mitigating effect on soil erosion since plants can protect the soil surface from rain or runoff detachment and reduce runoff velocity and sediment transport by intercepting raindrops, increasing soil permeability, increasing the roughness of the soil surface, and reinforcing soil mass stability (Bakker et al., 2005; Gyssels et al., 2005; Li et al., 1992b; Vannoppen et al., 2015). In most soil erosion models, vegetation is considered as an important factor influencing soil erosion rate (Morgan et al., 1998), and vegetation coverage is the parameter most commonly used to represent vegetation in models since it is easy to measure. (Duran Zuazo and Rodriguez Pleguezuelo, 2008; Labriere et al., 2015). Many studies have been conducted to look at the relationship between soil erosion rate and coverage under diverse environmental conditions, and these studies universally indicate that soil erosion rate decreases linearly or exponentially with coverage (Gyssels et al., 2005; Nearing et al., 2005). However, Gyssels et al. (2005) believed that the measured soil loss reduction resulted not only from coverage, or above-ground biomass, but also from the plant roots and soil properties. In many previous studies and soil erosion models, the effects of plant roots and soil properties on reducing soil detachment are attributed to the vegetation coverage due to the difficulty in excavating plant root in the field conditions (De Baets et al., 2006; Gyssels and Poesen, 2003; Wang and Zhang, 2017). In reality, vegetation coverage is only the most important factor in splash and inter-rill erosion, whereas in the process of rill erosion (mainly caused by

* Corresponding author at: State Key Laboratory of Soil Erosion and Dryland Farming on the Loess Plateau, Institute of Soil and Water Conservation, Northwest A&F University, Yangling, Shaanxi, 712100, PR China.
E-mail address: bwang@ms.iswc.ac.cn (B. Wang).

https://doi.org/10.1016/j.agee.2018.07.016
Received 8 May 2018; Received in revised form 18 July 2018; Accepted 21 July 2018

overland flow), plant roots play a much more important role in reducing soil detachment (Gyssels et al., 2005). Therefore, to better understand the mechanisms by which vegetation effects soil erosion, it is important to distinguish the role of plant roots and soil properties from that of vegetation coverage, and to quantify their distinct effects on reducing soil detachment.

The primary mechanisms by which plant roots reduce soil detachment are by reinforcing soil mass and improving soil shear strength (De Baets et al., 2006; Knapen et al., 2007; Herbrich et al., 2018). Soil generally has high compression strength but low tensile strength, whereas plant roots are the opposite (Simon and Collison, 2001, 2002). During the process of plant growth, the root interweaves into the soil mass (producing the soil-root matrix) and intensifies the soil's resistance to flowing water. (Gyssels et al., 2005; Reubens et al., 2007). This process is called the root binding effect as reported by Wang and Zhang (2017). Besides, the root bonding effect, which refers to how mucilage secretion of plant roots cause them to adhere to soil particles (via intermolecular bonding and Van der Waals forces), must also be considered, since it accounts for more than one quarter of the soil loss reduction caused by total plant root system (Wang et al., 2015). As mentioned by Li et al. (1991, 1992a), the soil's resistance to scouring is enhanced by plant roots, and this reduction of soil loss increases as "Effective Root Density" (the numbers of plant root with diameter less than 1 mm in a soil cross-sectional area of 100 cm^2) increases. The effects of plant roots on soil erosion also differs between various root types and root type architectures. Fibrous root systems generally have many fine roots, rather than one large roots and fewer fine roots, and this gives them an erosion-reducing potential that is much more significant than that of tap root systems. (Mamo and Bubenzer, 2001a,b). Wang and Zhang (2017) concluded that soil detachment capacity in grasslands with tap root systems was as much as 14.7 times higher than that of grasslands with fibrous root systems. Moreover, many studies have shown that soil loss rates decrease exponentially as root mass density, root length density, or root area ratio increase. This functional relationship has been applied in some soil erosion models, e.g. USLE and WEPP (Morgan et al., 1992; Nearing et al., 1991).

The growth or development of plant roots can affect the physical properties and nutrient levels of soil, which consequently affect soil erodibility (Islam and Weil, 2000; Schwarz et al., 2015; Xin et al., 2016). The effects of plant roots on soil properties can be summarized in terms of the following aspects: clumping fine soil particles together into firm macroaggregates and improving soil aggregate stability, interweaving with the soil and strengthening soil cohesion, extruding soil mass and changing soil bulk density, improving water movement and infiltration capacity, decomposing organic residues, and increasing soil organic matter (Gyssels et al., 2005; Li et al., 1991; McDonald et al., 2002; Zhang et al., 2017). Many previous studies have confirmed that soil bulk density, soil cohesion, soil aggregate stability (or water stable aggregate), and soil organic matter content are inversely proportional to soil detachment rate (Ghebreiyessus et al., 1994; Li et al., 2015; Morgan et al., 1998; Nearing et al., 1988; Wang et al., 2013). However, the effect of soil properties on soil erosion can also differ between different vegetation types. For example, large-diameter roots (those larger than the soil pores) can push soil particles aside and increase soil bulk density (Simon and Collison, 2001), while fine roots (those with diameter less than 1 mm) would decrease soil bulk density (Li et al., 1992b). Soils from the same area with similar soil textures can still have significantly different soil properties due to differences in community composition (Wang et al., 2018).

Mean annual soil erosion rates on the Loess Plateau range from 5000 to 10 000 tons km^{-2} yr^{-1} (Zhang and Liu, 2005), making it one of the most severely eroded regions in the world, and a series of ecological restoration projects have been implemented in this area to control soil erosion. For example: extensive tree planting on slope farmland in the 1970s, integrated soil erosion control at watershed scales in the 1980s and 1990s, and the "Grain for Green" project in 1999. As a result of these efforts, 41.7% (2.6×10^5 km^2) of the Loess plateau was grassland at the end of 2010, making grassland the primary land-use type in the region (Li et al., 2016). The communities, or dominant species of grasslands, differ between different areas of the plateau due to the differences in seed banks, succession pathways, and growth conditions during the process of vegetation succession (Jiao et al., 2012; Wang et al., 2018). Since they have significantly different root characteristics, these different plants have varying effects on the process of soil erosion, and though the influence of soil and root system properties on soil detachment have been quantified separately, the response of soil detachment to the various combinations of soil and root system properties have not been fully quantified and are in need of further study. Hence, ten typical grasslands with different root types and varied soil properties, reflecting different stages of vegetation succession on the Loess Plateau, were selected to: 1) study how the soil detachment process responds to various combinations of plant root and soil properties, 2) quantify the relationship between soil detachment capacity and root characteristics or soil properties, and 3) develop a model to estimate soil detachment capacity in grasslands based on flow hydraulic parameters, root characteristics, and soil properties.

2. Materials and methods

2.1. Study area and site selection

This study was carried out in the Zhifanggou watershed, which is located in the middle of the Loess Plateau (8.27 km^2; Ansai county; N36°46′28″to N36°46′42″, E109°13′03″to E109°16′46″; Fig. 1). The study area is a typical loess hilly-gully region. The area has a warm climate, and is in the transition region between semi-humid and semi-arid. The mean annual temperature and mean annual precipitation are 8.8 °C and 505 mm, respectively. The soil has a typical silt loam texture,

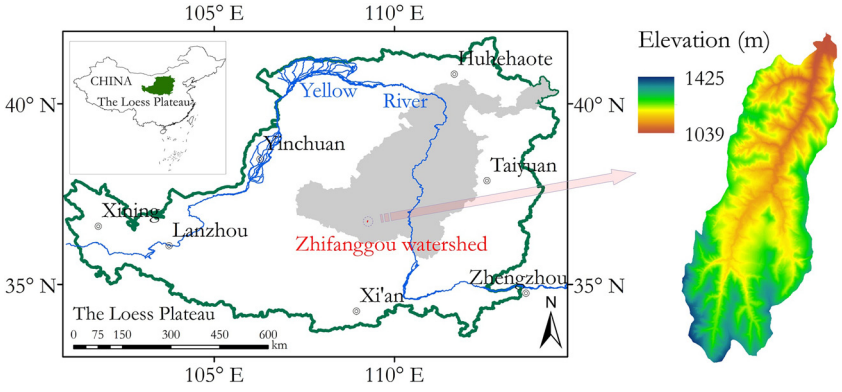

Fig. 1. Location of Zhifanggou watershed.

and the natural vegetation is characteristic of a forest steppe zone (Wang et al., 2018).

Ten typical grasslands, representing primary community compositions in the different stages of vegetation succession on the Loess Plateau, were selected for this study. In five of these grasslands, the dominant species have tap root systems (*Artemisia capillaris* Thunb., *Astragalus melilotoides* Pall., *Artemisia argyi* Levl. et Vant., *Artemisia vestita* Wall. ex Bess. and *Lespedeza davurica* (Laxm.) Schindl.), while the dominant species in the other five have fibrous root systems (*Poa sphondylodes* Trin., *Stipa bungeana* Trin., *Leymus secalinus* (Georgi) Tzvel., *Cleistogenes squarrosa* (Trin.) Keng. and *Bothriochloa ischcemum* (Linn.) Keng.). All of the selected grasslands had been used as farmlands but were abandoned after the implementation of a series of ecological restoration initiatives, thus each underwent a natural succession process. The slope gradients and aspects of the selected grasslands were similar, and the soil texture was a silt loam with little variation in clay, silt, and sand contents (which ranged from 9.3% to 14.5%, 61.6% to 72.6%, and 12.9 to 28.4%, respectively).

2.2. Sampling for soil detachment and soil properties measurement

The undisturbed soil samples for soil detachment measurement were taken from the top-soil layer (0 to 5 cm) for each grassland using steel rings with interior diameters of 9.8 cm and heights of 5 cm. In terms of details, the sampling process was the same as that described in Wang and Zhang (2017), with the exception that a single dominant herbage was selected for each sampling (by ensuring that the stem of the desired plant was in the center of the sampling ring) and its aboveground biomass was measured (65℃, 24 h). Each sample was sealed immediately with plastic wrap after sampling, and the mixed soil around each sampling point was collected to test soil moisture and to estimate the dry soil weight for the corresponding sample. In total, 300 soil samples were collected from ten grasslands for soil detachment capacity measurement. Meanwhile, the bulk density, soil aggregate, soil cohesion, and soil organic matter of each grassland were tested. These tests employed steel rings (5 cm in height, 5 cm in diameter); a series of sieves with the bore diameters of 0.25, 0.5, 1, 2, 3, 5, 8 and 10 mm; an Eijkelkamp pocket vane tester; and a measure of Potassium dichromate, respectively (mixed soil sample, “S” type sampling). Each test was repeated five times for each grassland, and the mean values by grassland are shown in Table 1.

2.3. Hydraulic parameters and soil detachment capacity measurement

Soil detachment capacity by overland flow was measured in a hydraulic flume measuring 4 m in length and 0.35 m in width. Before soil detachment was measured, six combinations of slope and unit flow discharge (17.5% and 0.003 m^2 s^{-1}, 17.5% and 0.006 m^2 s^{-1}, 26.2% and 0.006 m^2 s^{-1}, 43.6% and 0.004 m^2 s^{-1}, 43.6% and 0.006 m^2 s^{-1}, and 43.6% and 0.007 m^2 s^{-1}) were selected to obtain the corresponding shear stresses. Flow surface velocities were tested for each of the six combination of slope and flow discharge using a fluorescent dye method ($KMnO_4$). The tests were conducted within a 2 m interval at a distance of 0.6 m from the outlet of the flume, and they were replicated 3 times at each of 12 evenly distributed points across the flume cross section. The mean flow velocities under each combination (1.01, 1.30, 1.43, 1.58, 1.60 and 1.83 m s^{-1}) were calculated by multiplying a reduction factor which was determined by flow regime (Luk and Merz, 1992). Then, the flow depth (h, m; 2.9, 4.5, 3.9, 2.7, 3.7 and 4.0 × 10^{-3} m) and flow shear stress (τ, Pa; 4.98, 7.58, 10.01, 11.19, 15.24 and 16.37 Pa) were calculated using Eqs. (1) and (2). Stream power (ω, kg m^{-3}) and unit stream power (p, m s^{-1}) were also calculated using Eqs. (3) and (4).

$$h = \frac{Q}{vB} \tag{1}$$

$$\tau = \rho g h S \tag{2}$$

$$\omega = \tau v \tag{3}$$

$$p = Sv \tag{4}$$

where Q is the flow discharge (m^3 s^{-1}), v is the mean flow velocity (m s^{-1}), and B is the flume width, ρ is the density of water (kg m^{-3}), g is the constant of gravity (m s^{-2}), and S is the sine of the slope (m m^{-1}).

Before soil detachment capacity was measured, each soil sample was wetted for 8 h to eliminate the effects of soil water content on the measuring process. Then, the soil sample was laid in the flume bed, 0.6 m from the flume outlet, and scoured under the designed flow discharge and slope gradient. The test was replicated five times under each shear stress. The testing process was stopped when the scouring depth of the soil sample reached 2 cm, and the scouring time (which ranged between 2.22 s and 398.47 s) was recorded. A detailed description of the measurement process used in this study can be found in Wang and Zhang (2017). In total, 300 soil samples were tested and the soil detachment capacity (D_c, kg m^{-2} s^{-1}) of each sample was computed based on Eq. (5).

$$D_c = \frac{W_0 - W_a}{A \times t} \tag{5}$$

where W_0 is the dry weight of soil sample before scouring (kg), W_a is the dry weight of soil sample after scouring (kg), A is the scouring area (m^2), and t is the scouring time (s). For each shear stress, the mean D_c of the five replicates was calculated to reflect the effects of that shear stress on soil detachment.

2.4. Statistical analysis

Correlation analysis was utilized to analyze the correlation coefficient between soil detachment capacity and soil properties. A serious of fitted curves were used to quantify the relationships between aboveground biomass and root mass density, root mass density and soil organic matter, soil detachment capacity and hydraulic parameters, soil detachment capacity and soil properties, and soil detachment and root

Table 1
Soil properties of ten selected typical grasslands.

Site (code)	Bulk density (kg m^{-3})	Aggregate (> 0.5 mm, -)	Cohesion (K Pa)	Median soil grain size (D50) (μm)	Soil organic matter (g kg^{-1})
Artemisia capillaris Thunb. (HH)	852	0.47	5.16	33.32	6.57
Astragalus melilotoides Pall. (HQ)	837	0.49	5.13	34.67	6.98
Artemisia argyi Levl. Et Vant. (AH)	901	0.63	6.76	31.84	22.14
Artemisia vestita Wall. ex Bess. (TGH)	1048	0.84	8.66	20.51	7.71
Lespedeza davurica (Laxm.) Schindl. (HZZ)	1272	0.72	6.83	33.6	18.12
Poa sphondylodes Trin. (ZSH)	1029	0.72	7.74	22.54	11.36
Stipa bungeana Trin. (CMC)	1102	0.72	6.73	33.55	13.29
Leymus secalinus (Georgi) Tzvel. (BC)	1383	0.81	7.51	34.44	5.05
Cleistogenes squarrosa (Trin.) Keng. (YZC)	1152	0.72	7.55	34.88	8.35
Bothriochloa ischcemum (Linn.) Keng. (BYC)	1198	0.7	6.47	32.44	10.99

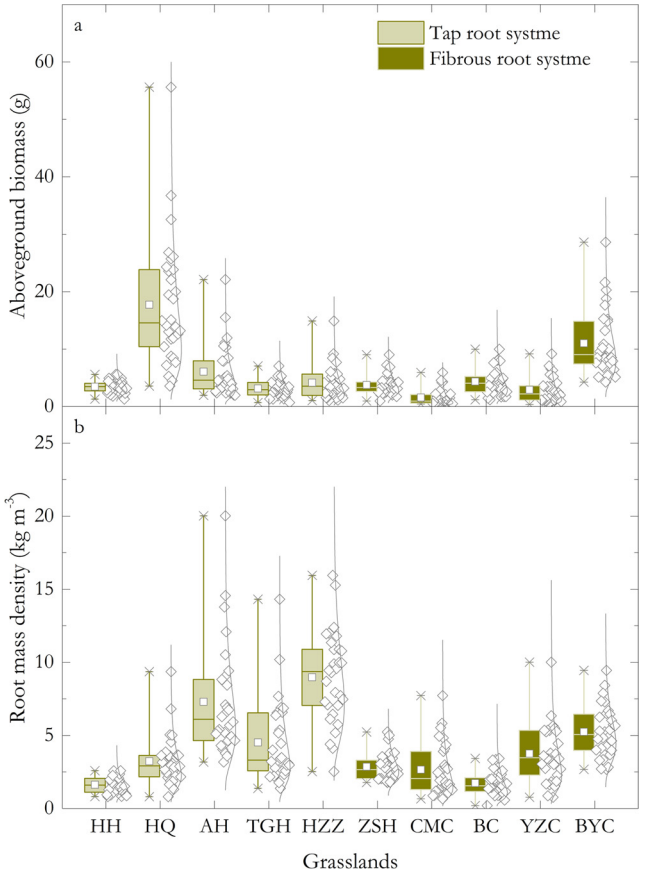

Fig. 2. Comparison of herbage characteristics between grasslands with tap and fibrous root systems. (a) aboveground biomass and (b) root mass density; HH, HQ, AH, TGH and HZZ are *Artemisia capillaris* Thunb., *Astragalus melilotoides* Pall., *Artemisia argyi* Levl. Et Vant., *Artemisia vestita* Wall. ex Bess., and *Lespedeza davurica* (Laxm.) Schindl., respectively. ZSH, CMC, BC, YZC and BYC are *Poa sphondylodes* Trin., *Stipa bungeana* Trin., *Leymus secalinus* (Georgi) Tzvel., *Cleistogenes squarrosa* (Trin.) Keng., and *Bothriochloa ischcemum* (Linn.) Keng., respectively.

mass density. Stepwise regression was used to estimate soil detachment capacity by hydraulic parameters, soil properties, and root mass density. The coefficient of determination (R^2) and Nash–Sutcliffe efficiency (*NSE*) were used to evaluate model performance. All analyses were done using SPSS 22.0 (IBM SPSS Statistics., 2013) and Origin Pro 8.0 (OriginLab Corp., 2008).

3. Results

3.1. Vegetation characteristics of ten typical grasslands

Aboveground biomass (AGB) and root mass density (RMD) varied significantly among the selected grasslands due to the significant differences between herbage species (Fig. 2a and b). Mean AGB by grassland varied from 1.58 g to 17.73 g per individual and the maximum (found in *Astragalus melilotoides* Pall.) was 11.2 times greater than the minimum (found in *Cleistogenes squarrosa* (Trin.) Keng.). Mean RMD ranged from 1.63 to 8.97 kg m^{-3}, and the maximum (found in *Lespedeza davurica* (Laxm.) Schindl.) was 5.5 times greater than the minimum (found in *Artemisia capillaris* Thunb.). The ratio of RM (root mass) to AGB (0 to 5 cm soil layer) ranged from 0.08 to 1.14 g g^{-1}, and the maximum (found in *Lespedeza davurica* (Laxm.) Schindl.) was 14.2 times greater than the minimum (found in *Astragalus melilotoides* Pall.). Vegetation characteristics also varied significantly with root type. For grasslands with tap root systems, the mean AGB, RMD and the ratio of

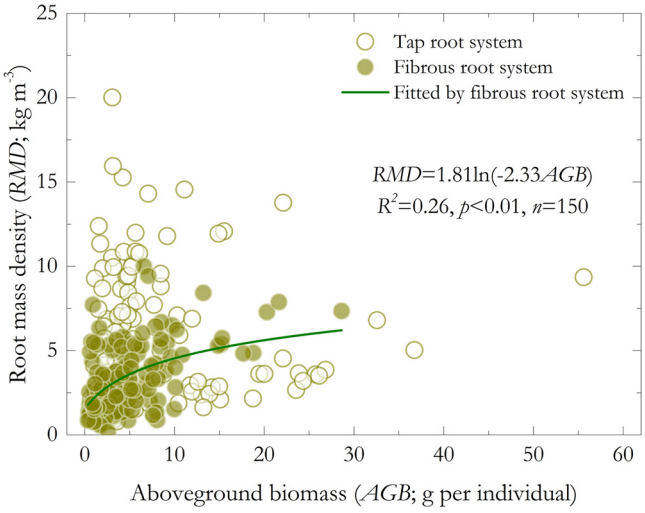

Fig. 3. Root mass density as a logarithmic function of aboveground biomass.

RM to AGB were 6.91 g per individual, 5.13 kg m^{-3} and 0.52 g g^{-1}, respectively, which were 1.5, 1.6 and 1.1 times greater than the corresponding means for grasslands with fibrous root systems. Moreover, a significant relationship between AGB and RMD was found in grasslands with fibrous root systems: RMD increased with AGB as a logarithmic function (R^2 = 0.26, p < 0.01; Fig. 3). No significant relationship between these values was found, however, in grasslands with tap root systems. This difference is probably due to the greater variety of root morphologies among plants with tap roots.

3.2. Differences in soil properties between the ten typical grasslands

Soil properties varied greatly between the ten typical grasslands, due mainly to the differences between herbage species and their root systems (Table 1). Soil bulk density (BD), soil aggregate (SA), and soil cohesion (COH) are commonly used to represent the effects of physical soil properties on soil erosion. Mean BDs by grassland ranged from 837 to 1383 kg m^{-3} and the maximum (found in *Leymus secalinus* (Georgi) Tzvel.) was 1.7 times greater than the minimum (found in *Astragalus melilotoides* Pall.). Mean SA and COH values ranged from 47.16 to 84.14% and 5.13 to 8.66 K Pa, respectively. *Artemisia vestita* Wall. ex Bess. had the maximum values for both SA and COH, which were 1.8 and 1.7 times greater than their respective minimums (found in *Artemisia capillaris* Thunb. and *Astragalus melilotoides* Pall., respectively). For soil organic matter (SOM), the mean values of ten test grasslands varied between 5.05 and 22.14 g kg^{-1}. The maximum SOM was found in *Artemisia argyi* Levl. Et Vant. and it was 4.4 times greater than the minimum, which was found in *Leymus secalinus* (Georgi) Tzvel. The ratio of maximum SOM to minimum SOM was much greater than the corresponding ratios for any of the physical soil properties, indicating that herbage species and their root systems have a particularly strong effect on soil organic matter. In addition, a significant power relationship was found between SOM and RMD (R^2 = 0.59, p < 0.01; Fig. 4), with SOM increasing as RMD increased. Greater differences in soil properties were also found between grasslands with tap root systems and those with fibrous root systems. For grasslands with tap root systems, the mean values of BD, SA and COH were 0.98 g cm^{-3}, 63.31%, and 6.51 K Pa, respectively, which were 16.3%, 13.8%, and 9.6% lower than the corresponding values for grasslands with fibrous root systems. Mean SOM across grasslands with tap root systems (12.30 g kg^{-1}) was 1.3 times greater than the corresponding value for grasslands with fibrous root systems. This difference was likely caused by the fact that much of the tap root mass was distributed relatively deep in the soil, and thus tap roots absorb less nutrient material from the top soil. The range of median soil grain sizes was small (D_{50}; ranged from 20.5 to

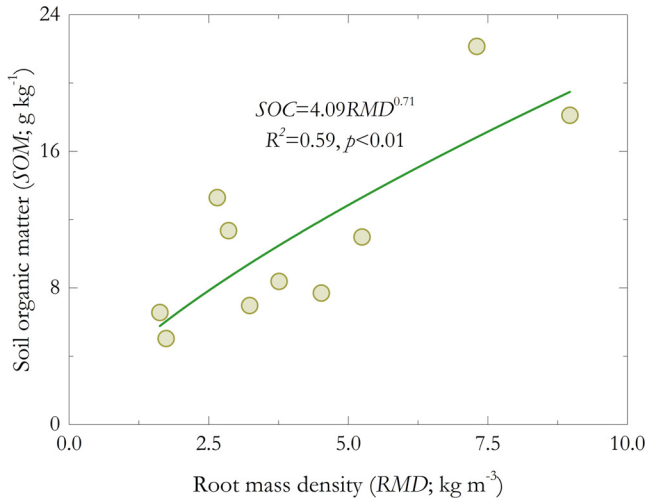

Fig. 4. Soil organic matter as a power function of root mass density.

34.9 μm) and the mean soil grain size across grasslands with tap root systems was only 2% less than the corresponding value for grasslands with fibrous root systems. This is because the soil texture of all ten grasslands was silt loam.

3.3. Variation in soil detachment among ten typical grasslands

Soil detachment capacity (D_C) varied significantly between the selected grasslands, largely due to the great differences in vegetation characteristics and soil properties between different sites. Mean values of D_C in different grasslands ranged from 0.030 to 3.297 kg m^{-2} s^{-1} (Table 2). For *Artemisia capillaris* Thunb. and *Astragalus melilotoides* Pall., mean values of D_C were 2.412 and 3.297 kg m^{-2} s^{-1}, respectively, which were 79.5 and 108.7 times greater than the minimum (found in *Poa sphondylodes* Trin. grasslands). *Artemisia capillaris* Thunb. is a pioneer species and usually appears in the early succession stage of the abandoned farmland. Therefore, soil erodibility in grasslands dominated by *Artemisia capillaris* Thunb. was high, which resulted in high soil detachment capacities. The root diameter of *Astragalus melilotoides* Pall. within the topsoil was coarse, and therefore it did little to reduce soil detachment. Mean soil detachment capacity (D_C) across grasslands with tap root systems was 1.180 kg m^{-2} s^{-1}, which was 14.7 times greater than the corresponding value for grasslands with fibrous root systems. This result demonstrates that herbage species with tap root system are less effective at reducing soil detachment capacity than those with fibrous root systems.

Table 2
Variations in soil detachment capacity of ten selected typical grasslands.

Site (code)	Soil detachment capacity (kg m^{-2} s^{-1})			
	Mean	Maximum	Minimum	*n*
Artemisia capillaris Thunb. (HH)	2.412	7.767	0.319	30
Astragalus melilotoides Pall. (HQ)	3.297	6.872	0.675	30
Artemisia argyi Levl. Et Vant. (AH)	0.085	0.535	0.021	30
Artemisia vestita Wall. ex Bess. (TGH)	0.051	0.105	0.014	30
Lespedeza davurica (Laxm.) Schindl. (HZZ)	0.056	0.225	0.019	30
Poa sphondylodes Trin. (ZSH)	0.030	0.093	0.011	30
Stipa bungeana Trin. (CMC)	0.121	0.330	0.024	30
Leymus secalinus (Georgi) Tzvel. (BC)	0.132	0.327	0.034	30
Cleistogenes squarrosa (Trin.) Keng. (YZC)	0.056	0.128	0.019	30
Bothriochloa ischcemum (Linn.) Keng. (BYC)	0.062	0.170	0.026	30

4. Discussion

4.1. Effects of hydraulics of overland flow on soil detachment

Overland flow was the driving force behind soil detachment. The hydraulic characteristics of overland flow (i.e. flow velocity, shear stress, stream power, and unit stream power) were closely related to soil detachment capacity. Some of these characteristics have been used in process-based erosion models to help simulate the soil detachment process (Nearing et al., 1999). The relationships between D_C and these four hydraulic parameters were analyzed, and the results show that the measured D_C of all ten tested grasslands increased with flow velocity, shear stress, stream power, and unit stream power as a series of power functions (Table 3; Fig. 5a–d). The performances of flow velocity (R^2 ranged from 0.72 to 0.98 with a mean of 0.88; NSE = 0.98), shear stress (R^2 ranged from 0.70 to 0.97 with a mean of 0.87) and stream power (R^2 ranged from 0.80 to 0.99 with a mean of 0.90) as predictors for D_C were all satisfactory, and no significant difference was found between these parameters. This result was consistent with previous studies which showed that flow velocity, shear stress, and stream power are good hydraulics parameter for simulating the process of soil detachment (Nearing et al., 1999; Wang et al., 2018). However, the performance of unit stream power as a predictor was relative poor, with a low coefficient of determination (R^2 ranged from 0.56 to 0.90 with a mean of 0.74).

4.2. Response of soil detachment to soil properties

Soil properties greatly affect the process of soil detachment and are widely used to quantify or estimate soil detachment capacity. In this study, the physical soil properties BD, SA, and COH were negatively correlated with D_C ($p < 0.01$, or $p < 0.05$; Table 4) and D_C decreased exponentially with BD, SA, or COH (Fig. 6a–c). In general, BD reflects the compactibility of soil mass. As BD increases, soil mass generally becomes more compact and soil cohesion is enhanced, which makes the soil mass more resistant to detachment by flowing water (Li et al., 2015). Similarly, a high SA promotes soil stability, increases soil resistance to flowing water erosion, and thus reduces soil detachment capacity (Wang et al., 2013). Some previous studies have indicated that the D_{50} (positively) and SOM (negatively) were both significantly correlated with D_C. Soil mass with a high D_{50} and low SOM would be easily scoured by flowing water because of its low cohesiveness (Ciampalini and Torri, 1998; Li et al., 2015). However, in this study D_C only showed a downward trend when D_{50} decreased and SOM increased. The relationships between the D_{50} or SOM alone and D_C were not significant ($p > 0.05$, Table 4). This is probably due to the fact that BD, SA, and COH all have much stronger effects on soil detachment.

4.3. Response of soil detachment to herbage root

Plant roots systems greatly affect the process of soil detachment, and their contribution to the reduction of soil detachment accounts for between half and two-thirds of the total contribution by all near soil surface factors (Wang et al., 2015). RMD is easy to measure and is commonly used to reflect the influence of plant roots on the process of soil detachment. In this study, the D_Cs of both grasslands with tap root systems and those with fibrous root systems decreased exponentially with RMD (for tap root system, $R^2 = 0.31$, $p < 0.01$; while for fibrous root system, $R^2 = 0.17$, $p < 0.01$; Fig. 7a and b). It is clear that the ability of soil mass to resist scouring by flowing water is enhanced by plant roots. The reticular root system can bind soil mass (binding effects) and the root exudates can adhere soil particles in the rhizosphere (bonding effects), which make soil structure more stable and resistant to detachment (Wang et al., 2015). The effects of plant roots on soil

Table 3
Regression results between soil detachment capacities (D_c; kg m^{-2} s^{-1}) and flow velocity, shear stress, stream power and unit stream power.

Site (code)	Velocity (v; m s^{-1})		Shear stress (τ, Pa)		Stream power (ω, kg s^{-3})		Unit stream power (p, m s^{-1})	
	Equation	R^2	Equation	R^2	Equation	R^2	Equation	R^2
Artemisia capillaris Thunb. (HH)	$D_c = 0.462v^{3.976}$	0.92	$D_c = 0.031\tau^{1.787}$	0.91	$D_c = 0.060\omega^{1.296}$	0.95	$D_c = 5.959p^{1.299}$	0.82
Astragalus melilotoides Pall. (HQ)	$D_c = 1.279v^{2.398}$	0.93	$D_c = 0.295\tau^{1.014}$	0.83	$D_c = 0.426\omega^{0.738}$	0.89	$D_c = 5.690p^{0.073}$	0.73
Artemisia argyi Levl. Et Vant. (AH)	$D_c = 0.022v^{3.330}$	0.91	$D_c = 0.002\tau^{1.535}$	0.97	$D_c = 0.004\omega^{1.099}$	0.98	$D_c = 0.179p^{1.037}$	0.83
Artemisia vestita Wall. ex Bess. (TGH)	$D_c = 0.018v^{2.651}$	0.98	$D_c = 0.004\tau^{1.089}$	0.85	$D_c = 0.005\omega^{0.806}$	0.93	$D_c = 0.092p^{0.767}$	0.79
Lespedeza davurica (Laxm.) Schindl. (HZZ)	$D_c = 0.032v^{1.461}$	0.75	$D_c = 0.010\tau^{0.713}$	0.89	$D_c = 0.014\omega^{0.492}$	0.86	$D_c = 0.078p^{0.411}$	0.56
Poa sphondylodes Trin. (ZSH)	$D_c = 0.011v^{2.448}$	0.88	$D_c = 0.002\tau^{1.045}$	0.82	$D_c = 0.004\omega^{0.764}$	0.87	$D_c = 0.050p^{0.646}$	0.59
Stipa bungeana Trin. (CMC)	$D_c = 0.053v^{2.109}$	0.72	$D_c = 0.009\tau^{1.075}$	0.89	$D_c = 0.016\omega^{0.727}$	0.84	$D_c = 0.210p^{0.703}$	0.71
Leymus secalinus (Georgi) Tzvel. (BC)	$D_c = 0.029v^{3.632}$	0.88	$D_c = 0.005\tau^{1.389}$	0.70	$D_c = 0.006\omega^{1.076}$	0.80	$D_c = 0.266p^{0.949}$	0.62
Cleistogenes squarrosa (Trin.) Keng. (YZC)	$D_c = 0.024v^{2.140}$	0.96	$D_c = 0.006\tau^{0.956}$	0.96	$D_c = 0.008\omega^{0.682}$	0.99	$D_c = 0.091p^{0.637}$	0.82
Bothriochloa ischcemum (Linn.) *Keng.* (BYC)	$D_c = 0.030v^{1.848}$	0.84	$D_c = 0.009\tau^{0.828}$	0.86	$D_c = 0.012\omega^{0.589}$	0.88	$D_c = 0.099p^{0.598}$	0.90

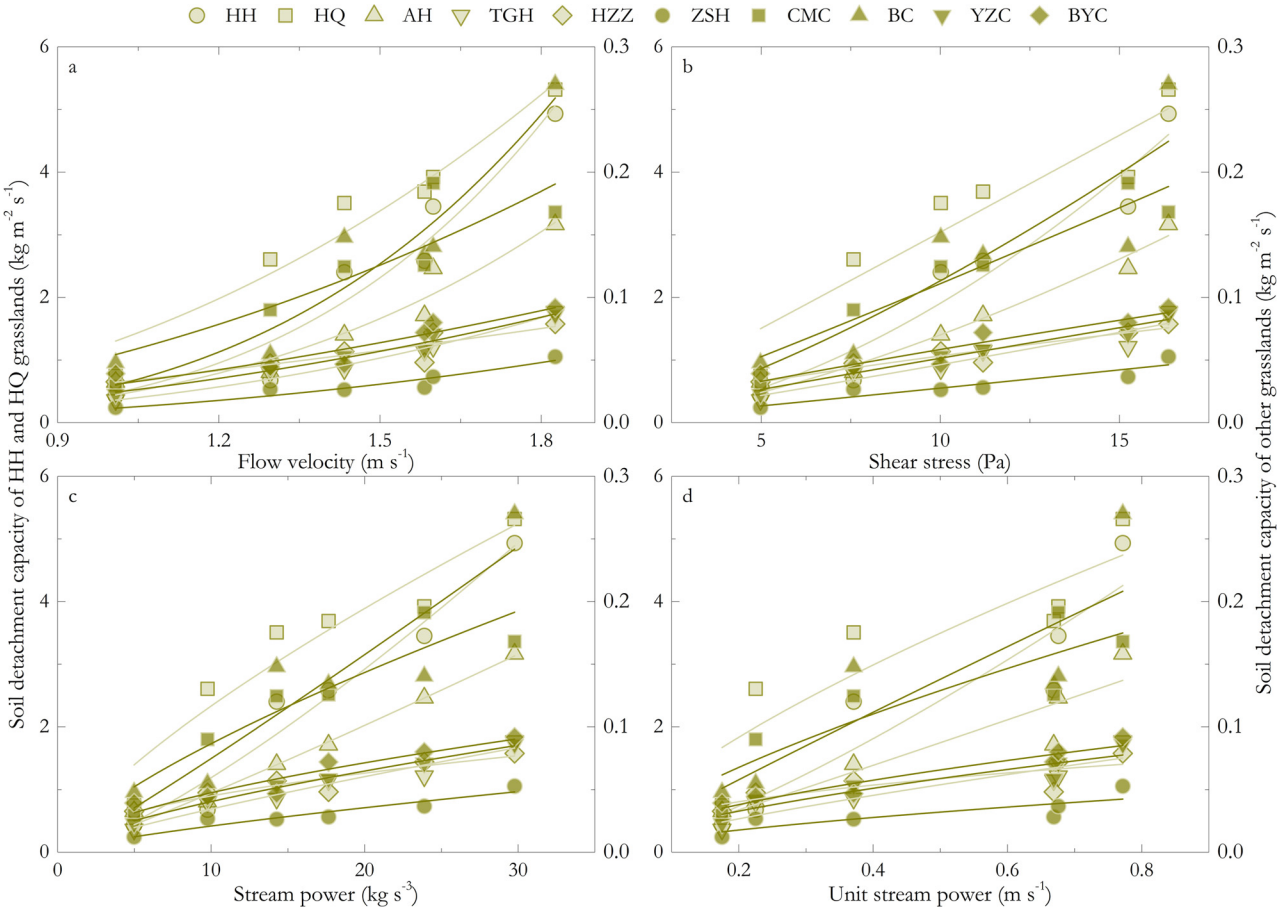

Fig. 5. Soil detachment capacity as power functions of hydraulic parameters. (a) flow velocity, (b) shear stress, (c) stream power and (d) unit stream power. Regression equations were listed in Table 3.

Table 4
Correlation coefficients between soil detachment capacity and soil properties.

Soil detachment capacity	Bulk density	Soil aggregate	Soil cohesion	Median soil grain size (D_{50})	Soil organic matter
	−0.664*	−0.854**	−0.809**	0.306	−0.406

Note: * $p < 0.05$; ** $p < 0.01$; $n = 10$.

detachment capacity is dependent on root structure. For grasslands with tap root systems, D_C decreased with RMD and declined rapidly in the root density range from 0 to 4 kg m^{-3}, which is consisted with the result of Zhang et al. (2013). Fibrous root systems were more effective than tap root systems at reducing soil detachment (the mean D_C the of former was 93.2% less than that of later) and, unlikely tap root systems, increased RMD in fibrous root systems continued to decrease soil detachment capacity steadily beyond the 4 kg m^{-3} mark.

4.4. Soil detachment capacity estimation

Since measuring soil detachment capacity in the field is time-consuming and costly, there is significant value in developing a model

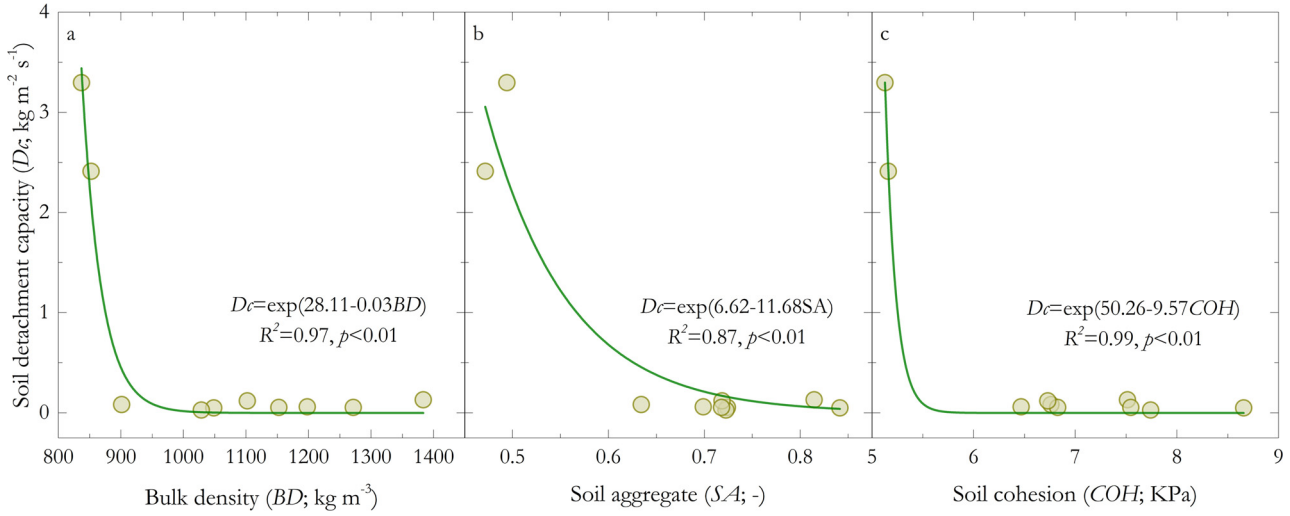

Fig. 6. Soil detachment capacity as an exponential function of soil properties. (a) bulk density, (b) soil aggregate and (c) soil cohesion.

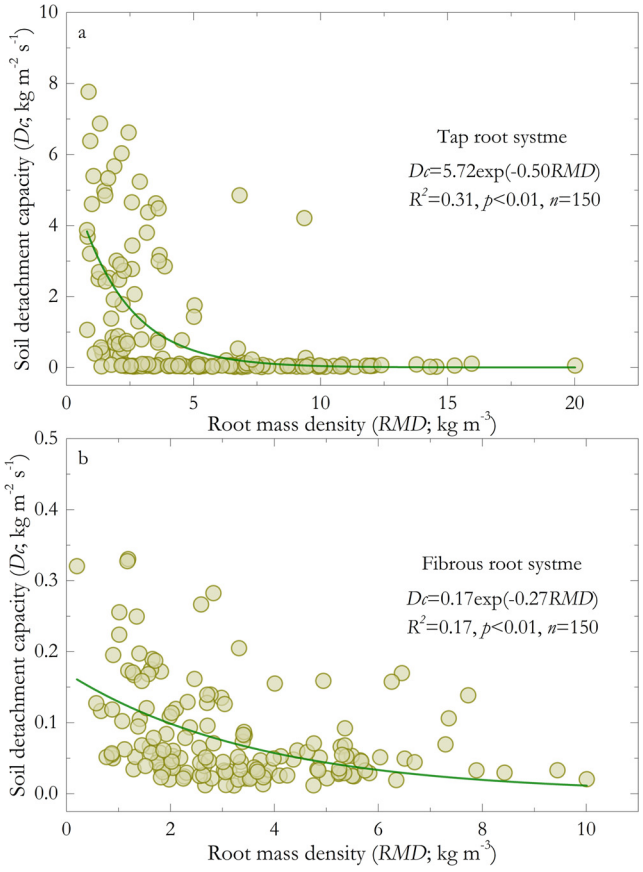

Fig. 7. Soil detachment capacity as exponential functions of root mass density. (a) grasslands with tap root system and (b) grasslands with fibrous root system.

which can be used to estimate soil detachment capacity based on hydraulics parameters, soil properties, and vegetation characteristics (Ciampalini and Torri, 1998; Li et al., 2015). In terms of model performance, no significant difference was detected between flow velocity, shear stress and stream power for simulating D_C. Shear stress is the most commonly used of these three parameters, hence it was selected for further analysis. In addition, the soil properties BD, SA, COH, and RMD were employed in the model.

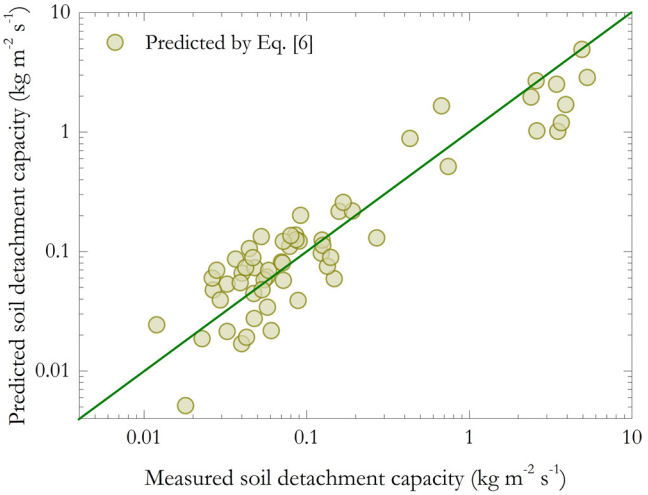

Fig. 8. Comparison between measured and predicted soil detachment capacity by Eq. (6).

$$D_c = 10^{1.551}\tau^{1.064}SA^{-3.043}COH^{-4.446}RMD^{-0.656} \quad (6)$$

The performance of Eq. (6) (R^2 = 0.86, NSE = 0.73) seemed satisfactory for simulating soil detachment capacity (Fig. 8). SA, COH, and RMD were primary factors influencing the process of soil detachment. BD was excluded during the process of stepwise regression, probably because of the positive correlation between BD and COH (Wang et al., 2013).

5. Conclusion

Several soil properties and of plant root characteristics, all of which vary between plant species and root types, seem to have an effect on the process of soil detachment. The mean soil detachment capacity of grasslands with tap root systems (1.180 kg m^{-2} s^{-1}) was 14.7 times great than that of grasslands with fibrous root systems, which suggests that the reduction of soil detachment capacity caused by grasslands with tap root systems is far less pronounced than that caused by grasslands with fibrous root systems. Coincidentally, the maximum and the minimum soil detachment were found in grasslands dominated by *Astragalus melilotoides* Pall. (3.297 kg m^{-2} s^{-1}; tap root system) and *Poa sphondylodes* Trin. (0.030 kg m^{-2} s^{-1}; fibrous root system) respectively. A series of power functions were fitted between soil detachment capacity and hydraulic parameters of overland flow. Flow velocity, shear

stress, and stream power were all good parameters for simulating soil detachment capacity, but unit stream power performed relatively poorly. Soil detachment capacity was significantly correlated to soil properties, and it decreased exponentially with bulk density, soil aggregate, and soil cohesion. In addition, the relationship between soil detachment capacity and root mass density could be described by a decreasing exponential function for both tap and fibrous root systems. In grasslands with tap root systems, a particularly rapid decline in soil detachment capacity occurred when the root mass density was less than 4 kg m^{-3}. Ultimately, it was found that soil detachment capacity on the Loess plateau could be estimated effectively by using hydraulic parameters of overland flow, plant root properties, and soil properties. The performance of the developed model was satisfactory ($R^2 = 0.86$; $NSE = 0.73$), and root mass density, soil aggregate, and cohesion were the primary factors influencing the process of soil detachment. Plants with tap root systems contributed less to the reduction of soil detachment capacity than plants with fibrous root systems. Since we know that most of root weight in tap root plants is found in the main root rather than the lateral roots, the hypothesis that the reduction in soil detachment capacity caused by tap root systems is due mostly to the lateral roots, rather than the tap root itself might bear further investigation.

Acknowledgments

Financial assistance for this work was supported by the National Natural Science Foundation of China (41530858 and 41771555), National Key Research and Development Plan (2016YFC0501703), the Innovative Talents Promotion Plan in Shaanxi Province (2017KJXX-88). We thank the Ansai Research Station of Soil and Water Conservation, the CAS & MWR for the technical assistance.

References

Bakker, M.M., Govers, G., Kosmas, C., Vanacker, V., van Oost, K., Rounsevell, M., 2005. Soil erosion as a driver of land-use change. Agric. Ecosyst. Environ. 105, 467–481.
Ciampalini, R., Torri, D., 1998. Detachment of soil particles by shallow flow: sampling methodology and observations. Catena 32, 37–53.
De Baets, S., Poesen, J., Gyssels, G., Knapen, A., 2006. Effects of grass roots on the erodibility of topsoils during concentrated flow. Geomorphology 76, 54–67.
Duran Zuazo, V.H., Rodriguez Pleguezuelo, C.R., 2008. Soil-erosion and runoff prevention by plant covers. A review. Agron. Sustain. Dev. 28, 65–86.
Ghebreiyessus, Y.T., Gantzer, C.J., Alberts, E.E., 1994. Soil-erosion by concentrated flow-shear-stress and bulk-density. Trans. ASAE 37, 1791–1797.
Gyssels, G., Poesen, J., 2003. The importance of plant root characteristics in controlling concentrated flow erosion rates. Earth Surf. Process. Landf. 28, 371–384.
Gyssels, G., Poesen, J., Bochet, E., Li, Y., 2005. Impact of plant roots on the resistance of soils to erosion by water: a review. Prog. Phys. Geogr. 29, 189–217.
Herbrich, M., Gerke, H.H., Sommer, M., 2018. Root development of winter wheat in erosion-affected soils depending on the position in a hummocky ground moraine soil landscape. J. Plant Nutr. Soil Sci. 181, 147–157.
Islam, K.R., Weil, R.R., 2000. Land use effects on soil quality in a tropical forest ecosystem of Bangladesh. Agric. Ecosyst. Environ. 79, 9–16.
Jiao, J., Zhang, Z., Bai, W., Jia, Y., Wang, N., 2012. Assessing the ecological success of restoration by afforestation on the Chinese Loess Plateau. Restor. Ecol. 20, 240–249.
Knapen, A., Poesen, J., Govers, G., Gyssels, G., Nachtergaele, J., 2007. Resistance of soils to concentrated flow erosion: a review. Earth. Rev. 80, 75–109.
Labriere, N., Locatelli, B., Laumonier, Y., Freycon, V., Bernoux, M., 2015. Soil erosion in the humid tropics: a systematic quantitative review. Agric. Ecosyst. Environ. 203, 127–139.
Li, Y., Zhu, X.M., Tian, J.Y., 1991. Effectiveness of plant roots to increase the anti-scourability of soil on the Loess Plateau. Chin. Sci. Bull. 24, 2077–2082.
Li, Y., Xu, X.Q., Zhu, X.M., 1992a. Preliminary-study on mechanism of plant-roots to increase soil antiscouribility on the Loess Plateau. Sci. China Ser. B–Chem. 35, 1085–1092.
Li, Y., Xu, X.Q., Zhu, X.M., Tian, J.Y., 1992b. Effectiveness of plant-roots on increasing the soil permeability on the Loess Plateau. Chin. Sci. Bull. 37, 1735–1738.
Li, Z.W., Zhang, G.H., Geng, R., Wang, H., Zhang, X.C., 2015. Land use impacts on soil detachment capacity by overland flow in the Loess Plateau, China. Catena 124, 9–17.
Li, J.J., Li, Z., Lu, Z.M., 2016. Analysis of spatiotemporal variations in land use on the Loess Plateau of China during 1986–2010. Environ. Earth Sci. 75.
Luk, S.H., Merz, W., 1992. Use of the slat tracing technique to determine the velocity of overlan-flow. Soil Technol. 5, 289–301.
Mamo, M., Bubenzer, G., 2001a. Detachment rate, soil erodibility, and soil strength as influenced by living plant roots part I: laboratory study. Trans. ASAE 44, 1167–1174.
Mamo, M., Bubenzer, G., 2001b. Detachment rate, soil erodibility, and soil strength as influenced by living plant roots part II: field study. Trans. ASAE 44, 1175–1181.
McDonald, M.A., Healey, J.R., Stevens, P.A., 2002. The effects of secondary forest clearance and subsequent land-use on erosion losses and soil properties in the Blue Mountains of Jamaica. Agric. Ecosyst. Environ. 92, 1–19.
Morgan, R., Quinton, J., Rickson, R., 1992. EUROSEM: Documentation Manual. Silsoe College, Silsoe, UK.
Morgan, R.P.C., Quinton, J.N., Smith, R.E., Govers, G., Poesen, J.W.A., Auerswald, K., Chisci, G., Torri, D., Styczen, M.E., 1998. The European Soil Erosion model (EUROSEM): a dynamic approach for predicting sediment transport from fields and small catchments. Earth Surf. Process. Landf. 23, 527–544.
Nearing, M.A., West, L.T., Brown, L.C., 1988. A consolidation model for estimating changes in rill erodibility. Trans. ASAE 31, 696–700.
Nearing, M.A., Bradford, J.M., Parker, S.C., 1991. Soil detachment by shallow flow at low slopes. Soil Scie. Soc. Am. J. 55, 339–344.
Nearing, M.A., Simanton, J.R., Norton, L.D., Bulygin, S.J., Stone, J., 1999. Soil erosion by surface water flow on a stony, semiarid hillslope. Earth Surf. Process. Landf. 24, 677–686.
Nearing, M.A., Jetten, V., Baffaut, C., Cerdan, O., Couturier, A., Hernandez, M., Le Bissonnais, Y., Nichols, M.H., Nunes, J.P., Renschler, C.S., Souchere, V., van Oost, K., 2005. Modeling response of soil erosion and runoff to changes in precipitation and cover. Catena 61, 131–154.
Reubens, B., Poesen, J., Danjon, F., Geudens, G., Muys, B., 2007. The role of fine and coarse roots in shallow slope stability and soil erosion control with a focus on root system architecture: a review. Trees–Struct. Funct. 21, 385–402.
Schwarz, M., Rist, A., Cohen, D., Giadrossich, F., Egorov, P., Buettner, D., Stolz, M., Thormann, J.J., 2015. Root reinforcement of soils under compression. J. Geophys. Res.–Earth Surf. 120, 2103–2120.
Simon, A., Collison, A.J.C., 2001. Pore-water pressure effects on the detachment of cohesive streambeds: seepage forces and matric suction. Earth Surf. Process. Landf. 26, 1421–1442.
Simon, A., Collison, A.J.C., 2002. Quantifying the mechanical and hydrologic effects of riparian vegetation on streambank stability. Earth Surf. Process. Landf. 27, 527–546.
Vannoppen, W., Vanmaercke, M., De Baets, S., Poesen, J., 2015. A review of the mechanical effects of plant roots on concentrated flow erosion rates. Earth. Rev. 150, 666–678.
Wang, B., Zhang, G.H., Shi, Y.Y., Zhang, X.C., Ren, Z.P., Zhu, L.J., 2013. Effect of natural restoration time of abandoned farmland on soil detachment by overland flow in the Loess Plateau of China. Earth Surf. Process. Landf. 38, 1725–1734.
Wang, B., Zhang, G.H., Shi, Y.Y., Li, Z.W., Shan, Z.J., 2015. Effects of near soil surface characteristics on the soil detachment process in a chronological series of vegetation restoration. Soil Sci. Soc. Am. J. 79, 1213–1222.
Wang, B., Zhang, G.H., Yang, Y.F., Li, P.P., Liu, J.X., 2018. The effects of varied soil properties induced by natural grassland succession on the process of soil detachment. Catena 166, 192–199.
Wang, B., Zhang, G.H., 2017. Quantifying the binding and bonding effects of plant roots on soil detachment by overland flow in 10 typical grasslands on the Loess Plateau. Soil Sci. Soc. Am. J. 81, 1567–1576.
Xin, Z., Qin, Y., Yu, X., 2016. Spatial variability in soil organic carbon and its influencing factors in a hilly watershed of the Loess Plateau, China. Catena 137, 660–669.
Zhang, X.C., Liu, W.Z., 2005. Simulating potential response of hydrology, soil erosion, and crop productivity to climate change in Changwu tableland region on the Loess Plateau of China. Agric. For. Meteorol. 131, 127–142.
Zhang, G.H., Tang, K.M., Ren, Z.P., Zhang, X.C., 2013. Impact of grass root mass density on concentrated flow erosion on steep slopes. Trans. ASABE 56, 927–934.
Zhang, F.B., Bai, Y.J., Xie, L.Y., Yang, M.Y., Li, Z.B., Wu, X.R., 2017. Runoff and soil loss characteristics on loess slopes covered with aeolian sand layers of different thicknesses under simulated rainfall. J. Hydrol. 549, 244–251.